Characterization of a buried neutral histidine residue in Bacillus circulans xylanase: NMR assignment, pH titration, and hydrogen exchange

ARTICLE *in* PROTEIN SCIENCE · NOVEMBER 1996

Impact Factor: 2.85 · DOI: 10.1002/pro.5560051118 · Source: PubMed

4 AUTHORS, INCLUDING:

Leigh A Plesniak

23 PUBLICATIONS **469** CITATIONS

SEE PROFILE

Protein Science (1996), 5:2319–2328. Cambridge University Press. Printed in the USA.

Characterization of a buried neutral histidine residue in *Bacillus circulans* xylanase: NMR assignments, pH titration, and hydrogen exchange

LEIGH A. PLESNIAK,[1,3] GREGORY P. CONNELLY,[1] WARREN W. WAKARCHUK,[2] AND LAWRENCE P. McINTOSH[1]

[1] Department of Biochemistry and Molecular Biology, Department of Chemistry, and the Protein Engineering Network of Centres of Excellence, University of British Columbia, Vancouver, British Columbia, Canada V6T 1Z3
[2] Institute for Biological Sciences, National Research Council of Canada, Ottawa, Ontario, Canada K1A 0R6

(RECEIVED July 5, 1996; ACCEPTED August 9, 1996)

Abstract

Bacillus circulans xylanase contains two histidines, one of which (His 156) is solvent exposed, whereas the other (His 149) is buried within its hydrophobic core. His 149 is involved in a network of hydrogen bonds with an internal water and Ser 130, as well as a potential weak aromatic–aromatic interaction with Tyr 105. These three residues, and their network of interactions with the bound water, are conserved in four homologous xylanases. To probe the structural role played by His 149, NMR spectroscopy was used to characterize the histidines in BCX. Complete assignments of the ^{1}H, ^{13}C, and ^{15}N resonances and tautomeric forms of the imidazole rings were obtained from two-dimensional heteronuclear correlation experiments. An unusual spectroscopic feature of BCX is a peak near 12 ppm arising from the nitrogen bonded $^{1}H^{\epsilon 2}$ of His 149. Due to its solvent inaccessibility and hydrogen bonding to an internal water molecule, the exchange rate of this proton (4.0×10^{-5} s^{-1} at pH* 7.04 and 30 °C) is retarded by $> 10^{6}$-fold relative to an exposed histidine. The pK_a of His 156 is unperturbed at ~6.5, as measured from the pH dependence of the ^{15}N- and ^{1}H-NMR spectra of BCX. In contrast, His 149 has a $pK_a < 2.3$, existing in the neutral $N^{\epsilon 2}H$ tautomeric state under all conditions examined. BCX unfolds at low pH and 30 °C, and thus His 149 is never protonated significantly in the context of the native enzyme. The structural importance of this buried histidine is confirmed by the destablizing effect of substituting a phenylalanine or glutamine at position 149 in BCX.

Keywords: hydrogen-deuterium exchange; imidazole; internal water; pH titration; pK_a; protein stability

Histidine is one of the most functionally versatile of the 20 naturally occurring amino acids found in proteins. Histidine residues often play key structural roles due to the planar aromatic nature of the heterocyclic imidazole side chain, with its ability to act both as a hydrogen bond donor and acceptor, as well as the positively charged member of a salt bridge. The pK_a of an imidazole ring falls near physiological pH, allowing the ionization state of this side chain to be modulated readily by its environment within a protein. The deprotonated nitrogen of an imidazole is also an effective ligand for metal ions. Perhaps most importantly, histidine residues serve critical enzymatic roles, functioning commonly in nucleophilic and general acid/base catalysis. Finally, the imidazole ring offers a wealth of spectroscopically obtainable information, allowing experimentalists to probe many details of the structure and function of histidine-containing proteins.

In this study, we report the characterization of the two histidine residues present in the xylanase from *Bacillus circulans*. BCX is a member of the family G or 11 low molecular weight endo-β-(1,4)-xylanases (Gilkes et al., 1991; Henrisaat & Bairoch, 1993; Davies & Henrissat, 1995). These enzymes catalyze the hydrolysis of xylan, an abundant structural heteropolysaccharide found in plant cell walls (Coughlan & Hazelwood, 1993). In a collaborative effort to develop BCX as a model β-glucanase and as a tool for potential applications in biotechnology, we and our co-workers have characterized extensively the stability, structure, and enzymology of this bacterial protein (Paice et al., 1986; Gebler et al., 1992; Wakarchuk et al., 1992, 1994a, 1994b; Campbell et al., 1993; Miao et al., 1994; Davoodi et al., 1995; Lawson et al., 1996; McIntosh et al., 1996; Plesniak et al., 1996).

Reprint requests to: L.P. McIntosh, Department of Biochemistry and Molecular Biology, 2146 Health Sciences Mall, University of British Columbia, Vancouver, BC, Canada, V6T 1Z3; e-mail: mcintosh@otter.biochem.ubc.ca.

[3] Present address: Chemistry Department, University of San Diego, San Diego, California 92110.

Abbreviations: BCX, *Bacillus circulans* xylanase; CT, constant-time; DSS, sodium 2,2-dimethyl-2-silapentane-5-sulfonate; HMBC, heteronuclear multiple-bond correlation; HSQC, heteronuclear single quantum correlation; MES, 2-(N-morpholino)ethanesulfonic acid; pH*, the pH meter reading without correction for isotope effects.

An interesting feature of the crystallographically determined structure of BCX is a histidine residue (His 149) that is buried completely within its hydrophobic core. The imidazole side chain of this residue stacked edge-on to a tyrosine ring (Tyr 105) and is involved in a network of hydrogen bonds to a nearby serine hydroxyl group (Ser 130) and a bound water molecule (Campbell et al., 1993). The histidine, serine, and tyrosine residues are absolutely conserved in all known Family G xylanases, as are the interactions between these groups and the bound water in the crystal structures of the related *Trichoderma harzianum* and *T. reesei* I and II xylanases (Campbell et al., 1993; Wakarchuk et al., 1994a; Törrönen et al., 1994; Törrönen & Rouvinen, 1995).[4] This suggests strongly that His 149 plays an important role in establishing the conformation of BCX, and thus is a potential target for mutagenesis to probe the stability of this xylanase. Conveniently, BCX also contains a nonconserved, solvent-exposed histidine at position 156 that serves an internal standard by which the properties of His 149 may be compared.

Using NMR spectroscopy, we have investigated the structural environments, pK_a values, and solvent accessibilities of these two histidine residues. Whereas His 156 behaves as expected for an unperturbed imidazole, His 149 is distinct in two key respects. First, it is highly protected from hydrogen exchange with the solvent, and second, its pK_a is <2.3 such that, at 30 °C, the imidazole side chain of this residue is never protonated significantly while buried within the interior of the folded enzyme. These comparisons illustrate dramatically how the properties of the two histidines depend on their structural contexts with this protein.

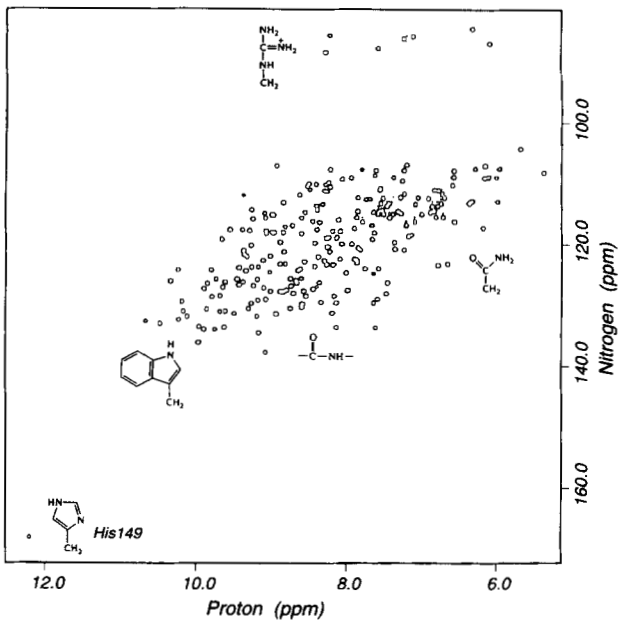

Fig. 1. ^{1}H-^{15}N HSQC spectrum of uniformly ^{15}N-labeled BCX. The sample contained 1 mM protein in 30 mM potassium chloride, 10 mM potassium phosphate buffer, pH* 4.0, at 30 °C. Approximate chemical shift ranges for the resonances from main-chain and side-chain amides, tryptophan indole $^{15}N^{\epsilon 1}H$, and arginine guanido $^{15}N^{\epsilon}H$ are indicated. The isolated peak at 12.19 ppm in ^{1}H and 168.3 ppm in ^{15}N arises from the $^{15}N^{\epsilon 2}H$ of the neutral buried imidazole ring of His 149.

Results

Identification of a buried histidine residue

The ^{1}H-^{15}N HSQC spectrum of BCX is presented in Figure 1. The spectrum of this 20.4-kDa protein is remarkably well dispersed, with almost every cross peak from the 178 main-chain and 23 side-chain amides, as well the 11 tryptophan indole and 7 arginine guanido groups, resolved. The assignments of the main-chain amide ^{1}H and ^{15}N resonances were obtained previously using three-dimensional triple resonance NMR experiments (Plesniak et al., 1996). Somewhat surprisingly, an isolated cross peak is observed in this HSQC spectrum with the distinct chemical shifts of 12.19 ppm in ^{1}H and 168.3 ppm in ^{15}N. The resonances contributing to this cross peak are also identified readily in the corresponding one-dimensional ^{1}H- and ^{15}N-NMR spectra of the protein (Fig. 2). As proven below, this cross peak arises from the imidazole $^{15}N^{\epsilon 2}H$ of His 149. In general, nitrogen bonded histidine protons, such as those of the exposed His 156 of BCX, are not observed in the ^{1}H-detected NMR spectra of proteins due to rapid exchange with the aqueous solvent. However, His 149 is entirely buried within BCX and thus exhibits significantly retarded hydrogen exchange kinetics.

Assignment of the histidine imidazole resonances

The downfield region of the one-dimensional ^{15}N-NMR spectrum of BCX under acidic conditions contains four peaks at the resonance frequencies of the imidazole ring nitrogens of His 149 and His 156 (Fig. 2). Based on the spectra of model compounds, the two peaks near 180 ppm correspond to the protonated nitrogens of an imidazolium cation, whereas those at 168.3 and 250.5 ppm arise from the protonated and nonprotonated nitrogens, respectively, of an uncharged imidazole (Blomberg et al., 1977; Blomberg & Rüterjans, 1983; Bachovchin, 1986; Witanoski et al., 1986; van Dijk et al., 1992; Pelton et al., 1993). Therefore, at pH < 5.5, one histidine side chain (His 149; see below) is unambiguously in the neutral form, whereas the other (His 156) is in the ionized state.

We completely assigned the resonances from the ^{1}H, ^{13}C, and ^{15}N nuclei in the imidazole rings of the two histidines in BCX using the following strategy (Figs. 3, 4).

1. The ring nitrogens were linked to their neighboring nonexchangeable $^{1}H^{\delta 2}$ and $^{1}H^{\epsilon 1}$ via weak two- and three-bond couplings detected in the ^{1}H-^{15}N HMBC spectrum of uniformly $^{13}C/^{15}N$-labeled BCX (Fig. 4A). The cross peak from directly bonded $^{15}N^{\epsilon 2}H$ of His 149 is also observed in this spectrum.

2. These nonexchangeable protons were connected to the directly bonded $^{13}C^{\delta 2}$ and $^{13}C^{\epsilon 1}$ by careful alignment of the ^{1}H-^{15}N HMBC spectrum with the constant-time ^{1}H-^{13}C HSQC spectrum recorded on the identical protein sample (Fig. 4B). Two features of the aromatic HSQC spectra of a uniformly 99% ^{13}C-labeled protein are worth highlighting with regard to the assignment of imidazole side chains. First, the $^{13}C^{\epsilon 1}$ of histidines are identified readily by their distinct downfield shifts and by the lack of carbon–carbon splittings in a regular HSQC spectrum recorded with suitable resolution in the ^{13}C dimension (not shown; Richarz & Wüthrich, 1978; Pelton et al., 1993).

[4] The Brookhaven Protein Data Bank codes are: *B. circulans* xylanase (1XNB), *T. harzianum* xylanase (1XND), *T. reesei* xylanase I (1XYN), and *T. reesei* xylanase II (1XYO & 1XYP).

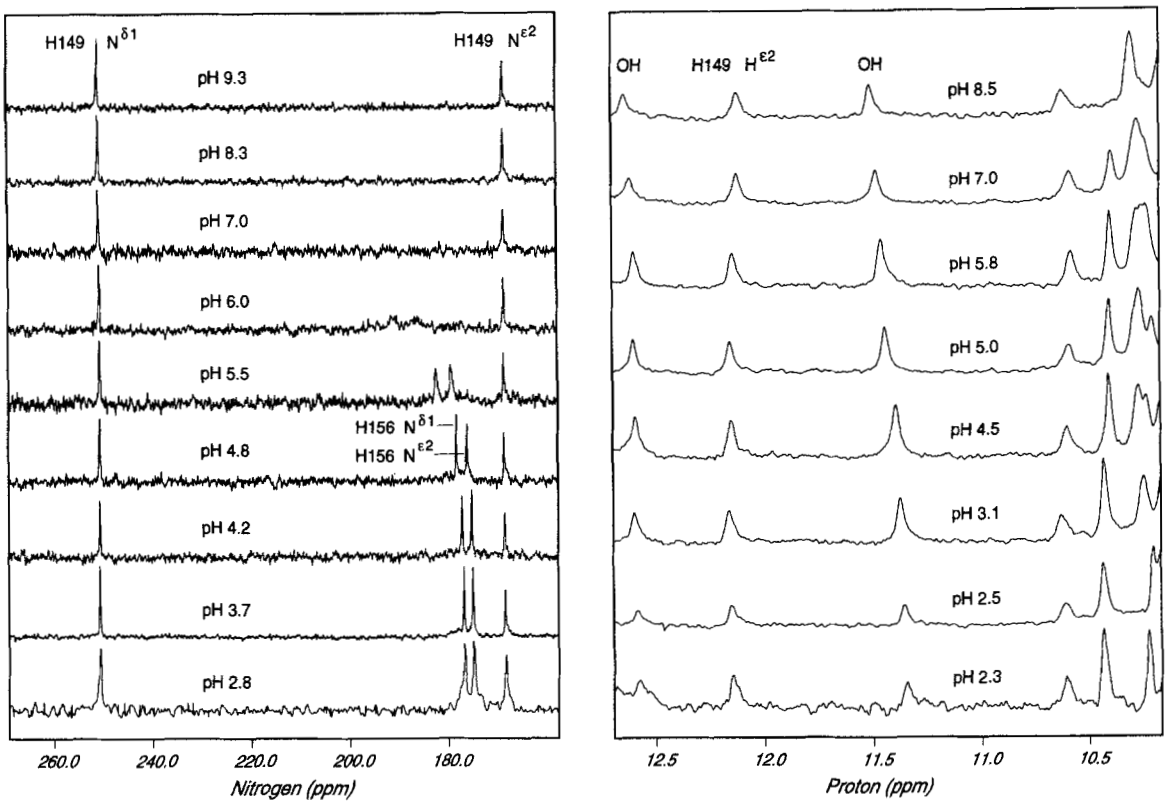

Fig. 2. Downfield regions of the one-dimensional ^{1}H-decoupled ^{15}N-NMR (left) and ^{15}N-decoupled ^{1}H-NMR spectra (right) of uniformly ^{15}N-labeled BCX recorded as a function of pH at 30 °C. Assignments of the peaks from His 149 and His 156 are indicated. The invariant chemical shifts of the $^{1}H^{\epsilon 2}$, $^{15}N^{\epsilon 2}$, and $^{15}N^{\delta 1}$ signals of His 149 indicate that the pK_a of this imidazole is <2.3 in the context of folded BCX. Peaks in the ^{1}H-NMR spectrum near 11.5 and 12.6 ppm likely arise from the phenolic O$^{\eta}$H of two of the many buried tyrosine side-chains found within BCX.

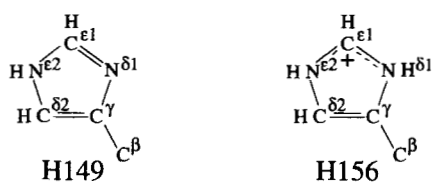

	$^{15}N\epsilon 2$	$^{1}H\epsilon 2$	$^{15}N\delta 1$	$^{13}C\delta 2$	$^{1}H\delta 2$	$^{13}C\epsilon 1$	$^{1}H\epsilon 1$	$^{13}C\beta$	$^{1}J_{N\epsilon 2H}$
His149	168.3	12.19	250.5	115.7	6.58	137.4	5.55	29.7	96 Hz
His156	182.6	--	186.4	121.5	7.01	137.8	8.36	28.9	--

Fig. 3. Summary of the predominant side-chain structures and chemical shift assignments (ppm) of His 149 and His 156 in BCX at 30 °C and pH* 5.8. Under these conditions, His 149 is in the neutral $N^{\epsilon 2}H$ form, whereas His 156 exists in an equilibrium between a major population of the charged imidazolium state and minor populations of the neutral $N^{\delta 1}H$ and $N^{\epsilon 2}H$ imidazole tautomers. Therefore, as evident from Figure 2, the reported ^{15}N chemical shifts of His 156 represent a weighted average of the chemical shifts of each of these possible protonation states. The specific assignments of the $^{15}N^{\delta 1}$ and $^{15}N^{\epsilon 2}$ resonances of His 156 are based on the relative intensities of the cross peaks observed in the ^{1}H-^{15}N HMBC spectrum of BCX (Fig. 4A).

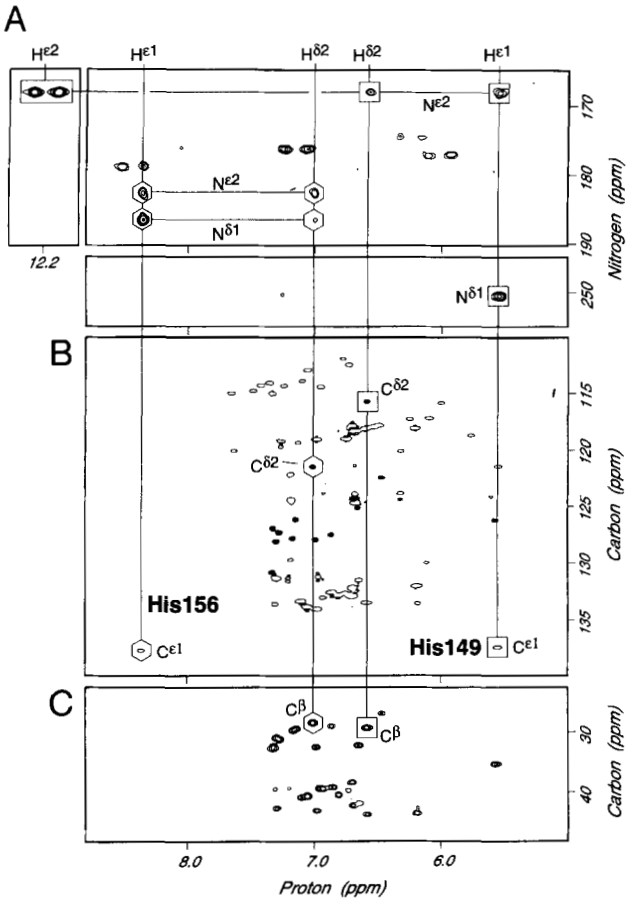

Fig. 4. Assignments of the ^{1}H, ^{13}C, and ^{15}N resonances of His 149 (squares) and His 156 (hexagons) were determined from the (**A**) ^{13}C-decoupled ^{1}H-^{15}N HMBC, (**B**) ^{15}N-decoupled constant-time ^{1}H-^{13}C HSQC, and (**C**) (Hβ)Cβ(CγCδ)Hδ spectra of uniformly $^{13}C/^{15}N$-labeled BCX at pH* 5.8 and 30 °C. The HMBC spectrum consists of three panels to cover the relevant chemical shift ranges. The directly bonded $^{15}N^{\epsilon 2}H$ of His 149 and the aliased $^{15}N^{\epsilon}H$ of the arginine side chains are doublets in the proton dimension because nitrogen decoupling was not applied during the acquisition period of the HMBC experiment. Inverted peaks in the constant-time ^{1}H-^{13}C HSQC, due to the $^{13}C^{\delta 2}H$ of His 149 and His 156 and the $^{13}C^{\delta 1}H$ of the 11 tryptophan residues, are filled in black. Contours are not shown for the positive peaks in B.

Second, the $^{13}C^{\delta 2}$ of histidine and the $^{13}C^{\delta 1}$ of tryptophan are unique among the aromatic side chains in that they have only one neighboring carbon atom. Thus, in a CT-HSQC spectrum recorded with a total constant-time delay of $1/^{1}J_{CC}$, the peaks from these carbons are inverted in sign relative to those from the remaining ring carbons with an even number of neighboring ^{13}C nuclei. Based on these simple patterns, we identified unambiguously the resonance of $^{1}H^{\epsilon 1}$ of His 149 lying *upfield* of the resonance from $^{1}H^{\delta 2}$. This is opposite to that expected from the random coil ^{1}H chemical shifts of imidazole rings (Bundi & Wüthrich, 1979), and thus highlights the utility of the ^{1}H-^{13}C CT-HSQC in assigning the NMR spectra of histidine residues. The unusual shift of the $^{1}H^{\epsilon 1}$ of His 149 is attributed to an aromatic ring current effect from the side chain of Tyr 105 (Fig. 7).

3. The nuclei in the imidazole rings were connected to those in the protein backbone based on $^{1}H^{\delta 2}$-$^{13}C^{\beta}$ correlations detected in the (Hβ)Cβ(CγCδ)Hδ spectrum of $^{13}C/^{15}N$-labeled BCX (Fig. 4C; Yamazaki et al., 1993). This approach relies on the large one-bond ^{1}H-^{13}C and ^{13}C-^{13}C scalar couplings, thus avoiding possible ambiguities associated with the conventional method of assigning aromatic rings using NOE interactions (Wüthrich, 1986). The $^{13}C^{\beta}$ chemical shifts of His 149 and His 156 were identified previously (Plesniak et al., 1996), thereby completing the assignment of the imidazole side chains of these two residues.

Assignment of the histidine tautomeric states

His 156 is protonated at pH < 5.5, with both ^{15}N nuclei having chemical shifts diagnostic of a charged imidazolium ring. As discussed clearly in the literature (Blomberg et al., 1977; Blomberg & Rüterjans, 1983; Pelton et al., 1993), the two- and three-bond couplings between the ring nitrogens and carbon bonded protons in the cationic imidazolium ring are all greater than 3 Hz in magnitude. Thus, all four possible correlations between $^{15}N^{\delta 1}/^{15}N^{\epsilon 2}$ and $^{1}H^{\delta 2}/^{1}H^{\epsilon 1}$ are observed in the ^{1}H-^{15}N HMBC spectrum of His 156 (Fig. 4A). However, inspection of these data reveals that the cross peak at 7.01 ppm and 186.4 ppm is clearly weaker than the remaining three. Given that the magnitude of the $^{3}J_{N\delta 1\text{-}H\delta 2}$ coupling constant is less than those of the three possible $^{2}J_{NH}$ couplings in a protonated histidine ring, we tentatively assign the nitrogen peaks at 182.6 and 186.4 ppm to $^{15}N^{\epsilon 2}$ and $^{15}N^{\delta 1}$ of His 156, respectively.

His 149 exists in the neutral state with its ^{15}N nuclei resonating at 168.3 and 250.5 ppm. In contrast to the case of the protonated imidazole ring, the magnitude of the three-bond $^{3}J_{N\delta 1\text{-}H\delta 2}$ coupling constant coupling is ~2 Hz. Thus, a cross peak between $^{15}N^{\delta 1}$ and $^{1}H^{\delta 2}$ is expected to be very weak or absent in the ^{1}H-^{15}N HMBC spectrum (Pelton et al., 1993). Based on this criterion, the peak at 250.5 ppm is assigned to the $^{15}N^{\delta 1}$ of His 149, and that at 168.3 ppm of the $^{15}N^{\epsilon 2}$. Therefore, His 149 exists in the tautomeric form with $^{15}N^{\epsilon 2}$ protonated, and the downfield peak observed at 12.19 ppm and 168.3 ppm in the ^{1}H-^{15}N HSQC spectrum of BCX is assigned unambiguously to $^{15}N^{\epsilon 2}H$. This assignment is supported further by the observation of NOE cross peaks of equal intensity between this nitrogen bonded proton and the adjacent $^{1}H^{\delta 2}$ and $^{1}H^{\epsilon 1}$ of His 149 in the NOESY spectrum of BCX, combined with the absence of cross peaks to the $^{1}H^{\beta,\beta'}$ of this residue (Figs. 5, 7) (Stoesz et al., 1979; Wu et al., 1984).

We also attempted to assign the tautomeric state of His 149 by recording high-resolution ^{1}H-^{13}C HSQC spectra of the ^{15}N- and ^{13}C-labeled protein with selective ^{15}N decoupling during the t_1 period. However, the $^{1}J_{NC}$ couplings were not resolved sufficiently to detect confidently changes in the linewidths of the $^{13}C^{\delta 2}$ and $^{13}C^{\epsilon 1}$ peaks with decoupling. An alternative assignment strategy would involve using a multidimensional NMR experiment to observe carbon bonded protons while providing indirectly the correlations between neighboring ^{15}N and ^{13}C nuclei.

pH titrations of the histidine residues in BCX

The chemical shifts of the ^{1}H, ^{13}C, and ^{15}N nuclei of histidines are dependent on the ionization state of the imidazole ring. Traditionally, this has provided a convenient avenue to measure experimentally the pK_a values of histidine side chains in proteins (Markley, 1975; Blomberg et al., 1977). Due to the relatively large size of BCX, the nonexchangeable $^{1}H^{\delta 2}$ and $^{1}H^{\epsilon 2}$ of His 149 and His 156

have resonances overlapping those of the many aromatic side chains in the protein. Combined with the difficulty in reversibly unfolding BCX to fully exchange the amide protons for deuterons (unpubl. obs.; Lawson et al., 1996), this precluded the use of ^{1}H-NMR to monitor the titrations of these two carbon bonded protons. An alternative method is to follow the titration of the histidines using the ^{1}H-^{13}C HSQC experiment (Yu & Fesik, 1994). However, this requires the use of an expensive isotopically labeled BCX sample, which may denature irreversibly under very acidic or basic conditions. Therefore, we focused our attention on the ^{15}N nuclei of the histidine rings.

The downfield regions of the ^{1}H- and ^{15}N-NMR spectra of BCX, recorded as a function of pH, are presented in Figure 2. At pH < 5.5, His 156 is clearly protonated with both ^{15}N resonating near 175 ppm. With increasing pH, these two peaks initially shift downfield, subsequently broadening beyond detection as the ring deprotonates. The broadening is attributed to protonation–deprotonation, coupled with interconversion of the tautomeric states of His 156, that occurs on the time scale of intermediate chemical exchange. If His 156 deprotonated to a single or predominant tautomeric form, the resonance of one ^{15}N should shift downfield to ~250 ppm, whereas the other would be expected to move upfield slightly to ~167 ppm (Blomberg & Rüterjans, 1983; Bachovchin, 1986). Based on the chemical shift changes measurable for the ^{15}N nuclei of His 156, we estimate that the pK_a of this residue is approximately 6.5. This is within the range expected for an exposed histidine in an unperturbed or random coil environment (Tanokura, 1983; Creighton, 1993).

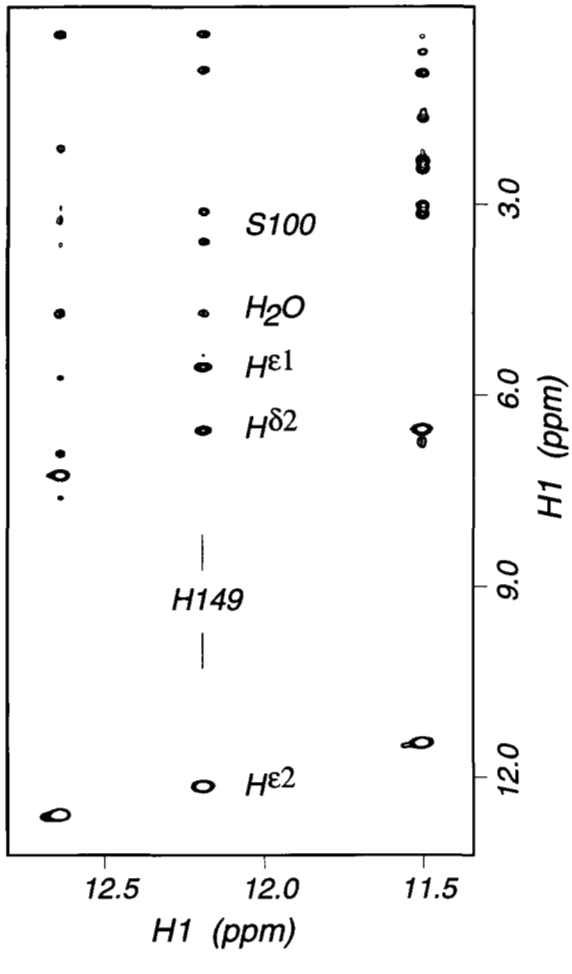

Fig. 5. Portion of the NOESY spectrum of BCX (τ_{mix} = 150 ms) recorded with a gradient 11-echo detection pulse sequence tuned for the ^{1}H$^{\epsilon 2}$ of His 149 (Sklenár & Bax, 1987). Assignment of the tautomeric state of His 149 is confirmed by NOE cross peaks between ^{1}H$^{\epsilon 2}$ and the adjacent carbon bonded ^{1}H$^{\delta 2}$ and ^{1}H$^{\epsilon 1}$ of this residue, as well as by the absence of NOEs to its ^{1}H$^{\beta,\beta'}$ (Plesniak et al., 1996). NOE cross peaks to the ^{1}H$^{\beta}$ and ^{1}H$^{\beta'}$ of nearby Ser 100 are also labeled. A cross peak at the frequency of H_2O is tentatively assigned to a NOE interaction with a buried water that is hydrogen bonded to N$^{\epsilon 2}$H of His 149 or to the O$^{\gamma}$H of Ser 100. The diagonal peaks at 11.5 and 12.6 likely arise from the phenolic O$^{\eta}$H of tyrosines.

In contrast to His 156, the buried His 149 is deprotonated under *all* pH conditions examined (Fig. 2). This conclusion follows from the observation that the chemical shifts of the ^{15}N$^{\epsilon 2}$, ^{15}N$^{\delta 1}$, and ^{1}H$^{\epsilon 2}$ of this residue are invariant between pH 9.3 and 2.3, showing that His 149 remains in one neutral tautomeric state even under very acidic conditions (cf. Patel et al., 1972; Zhong et al., 1995). Therefore, the pK_a of His 149 in native BCX is less than 2.3. However, under solution conditions more acidic than pH 3, BCX begins to unfold on the NMR timescale of slow exchange. This is evident by the appearance of resonances with random coil shifts (not shown) and a concomitant loss in the relative intensity of the peaks from the native protein (Fig. 2). Therefore, the pK_a of His 149 is less than the "midpoint pH" for the acid denaturation of BCX at 30 °C, such that this residue is not protonated significantly within the structural context of the folded protein.

Hydrogen-deuterium exchange of His 149

Insights into the structure and dynamics of proteins can be obtained by measurement of the rates by which labile protons exchange with solvent protons. In general, hydrogen exchange studies have focused on the main-chain amide and side-chain amide and indole groups in proteins. However, similar approaches may be used to probe the environment of His 149. Figure 6 presents the time course of exchange measured by transferring protonated BCX into D_2O buffer at pH* 7.04 and 30 °C, followed by recording a series of one-dimensional ^{1}H-NMR spectra. Remarkably, the rate of hydrogen-deuterium exchange of His 149 ^{1}H$^{\epsilon 2}$ under these conditions is 4.0×10^{-5} s^{-1}. In contrast, the nitrogen bonded protons of His 156 are not detected in the ^{1}H-NMR spectrum of BCX over the wide pH range studied. Assuming a conservative limit of ~100 Hz in the linewidth of an observable NMR signal, we estimate that these two exposed protons exchange with the water at a rate >300 s^{-1} at neutral pH (Wüthrich, 1986).

Close proximity of His 149 to a buried water or hydroxyl group

Inspection of the crystallographic structure of BCX reveals that His 149 is strongly hydrogen bonded to a buried water molecule via its N$^{\epsilon 2}$H (Fig. 7) (Campbell et al., 1993). The water O to His ^{1}H$^{\epsilon 2}$ separation is 1.8 Å. In an initial effort to confirm this interaction, we recorded a NOESY spectrum with a spin-echo detection pulse (Sklenár & Bax, 1987) to avoid saturating the solvent signal. As shown in Figure 5, an NOE cross peak is observed from a proton(s) with the chemical shift of bulk H_2O to His 149 ^{1}H$^{\epsilon 2}$. Because the lifetime for hydrogen exchange rate of this histidine proton is on the order of hours, this cross peak cannot be due to direct chemical exchange with water. We tentatively assign this cross peak to an NOE interaction between ^{1}H$^{\epsilon 2}$ of His 149 and

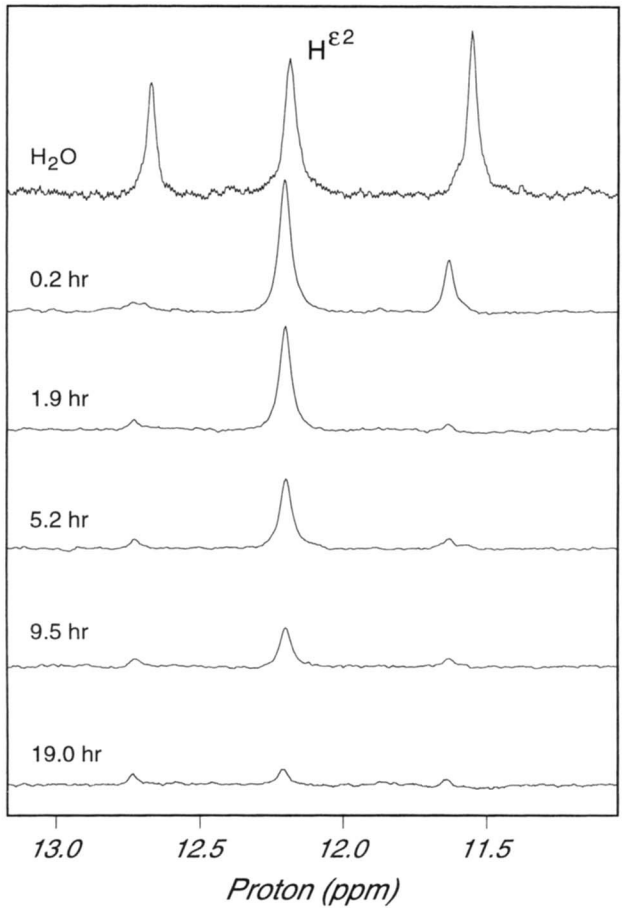

Fig. 6. Time course of the hydrogen–deuterium exchange of the $^1H^{\epsilon 2}$ of His 149 at 30 °C and pH* 7.04. The top spectrum corresponds to BCX in H_2O buffer, whereas the descending spectra were recorded after transfer into D_2O, with data acquisition started at the indicated times. Small peaks in the final spectrum result from ~5% residual HDO in the solvent.

either the bound water molecule or the $O^\gamma H$ of Ser 100. The latter O^γ and H^γ are 3.5 Å and 3.2 Å, respectively, from the imidazole $^1H^{\epsilon 2}$. It is interesting to note that this bound water and/or serine hydroxyl are likely in fast exchange with the solvent on the NMR timescale, as evident by a chemical shift coinciding with that of bulk water (Otting & Wüthrich, 1989; Otting et al., 1991).

Discussion

Structural environment of His 149

BCX contains two histidines at positions 149 and 156. His 149 is located on the interior of the single amphiphatic α-helix in BCX, resulting in its complete burial within the hydrophobic core of the protein (Fig. 7). The imidazole is almost perpendicular to the phenolic group of Tyr 105, such that the $H^{\epsilon 1}$ of His 149 points directly toward the C^γ on the face of this aromatic ring ($d_{149H\epsilon 1\text{-}105C\gamma}$ = 2.7 Å). This orthogonal edge-to-face stacking is suggestive of an aromatic–aromatic interaction in which the slightly positive proton of the histidine is attracted weakly to the slightly negative carbon atoms of the tyrosine ring (Burley & Petsko, 1988; Armstrong et al., 1993). The close proximity of His 149 to the aromatic ring of Tyr 105 undoubtedly results in the abnormally upfield shifted resonance of its imidazole $^1H^{\epsilon 1}$ at 5.55 ppm, versus 7.75 ppm expected for a neutral "random-coil" histidine (Fig. 4) (Bundi & Wüthrich, 1979).

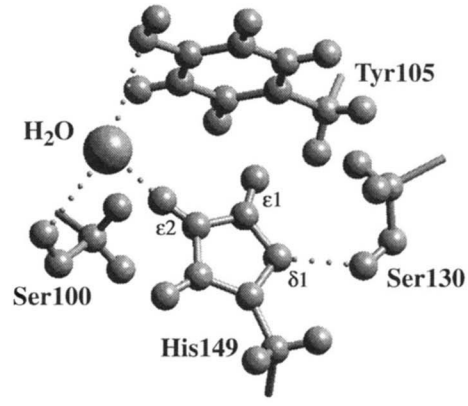

Fig. 7. Structural environment of His 149 observed in the crystal structure of BCX (Campbell et al., 1993). His 149 is hydrogen bonded (dotted line) to the $O^\gamma H$ of Ser 130 via its $N^{\delta 1}$ and to the oxygen of an internal water via its $N^{\epsilon 2}H$. The labile $H^{\epsilon 2}$ is protected from exchange with bulk solvent due to its buried, hydrogen bonded location within the protein. The imidazole side chain is stacked edge-to-face with the aromatic ring of Tyr 105, resulting in the strongly upfield shifted resonance observed for the carbon bonded $H^{\epsilon 1}$ of His 149. In addition to this histidine, the internal water is hydrogen bonded to the side chains of Ser 100, Tyr 105, and Asp 101 (not shown). The figure was generated with SETOR (Evans, 1993), and hydrogen atoms were added using InsightII (Biosym, Inc.).

In the crystal structure of BCX, His 149 is hydrogen bonded to the oxygen of an internal water molecule and the hydroxyl proton of Ser 130 via its $N^{\epsilon 2}H$ and $N^{\delta 1}$, respectively (each with N-O distances of 2.8 Å) (Campbell et al., 1993). However, because nitrogen and carbon atoms are difficult to distinguish by X-ray crystallography, and protons are generally not observed in electron density maps, the orientation and tautomeric state of this imidazole ring were deduced based on the observed positions of neighboring polar atoms. Using NMR methods, we have confirmed unambiguously that His 149 exists in the $N^{\epsilon 2}H$ tautomeric form, thereby providing strong independent support for the hydrogen bonding interactions reported in the structural model of BCX. The NOEs observed between the $^1H^{\epsilon 2}$ of His 149 and the nearby $^1H^{\beta,\beta'}$ of Ser 100, as well as a bound water or the hydroxyl of this latter serine, are also entirely consistent with the crystal structure of the protein.

Structural environment of His 156

In contrast to His 149, the nonconserved His 156 is located at the C-terminal end of the α-helix in BCX with its imidazole $N^{\delta 1}$ hydrogen bonded to the carbonyl oxygen of Ala 152. The following residue, Gly 157, which is invariant in all Family G xylanases, serves as the C-cap of the α-helix (Richardson & Richardson, 1988; Campbell et al., 1993). The side chain of His 156 is solvent accessible and does not neighbor closely any other ionizable amino acids in BCX. Consistent with this exposed structural environment, the nitrogen bonded protons of His 156 exchange rapidly with water and the $pK_a \sim 6.5$ of its side chain is within the range expected for a typical histidine residue located on the surface of a protein (Creighton, 1993).

It is interesting that Sancho et al. (1992) have shown that the pK_a of His 18 in the C-cap position of an α-helix in barnase is

elevated by 0.6 units to 7.1 due to favorable electrostatic interactions of the imidazole ring with the helix dipole combined with hydrogen bonding to the carbonyl oxygen of residue $i - 3$ (Gln 15). This hydrogen bonding protects the imidazole of His 18 sufficiently from solvent exchange such that the nitrogen bonded protons are observable by NMR using a selective pulse sequence to avoid saturation of bulk water (Sancho et al., 1992). Keeping in mind that we did not detect the full titration curve of His 156 in native BCX and did not measure its pK_a in the unfolded protein, it is possible that the pK_a of this residue is elevated slightly from a "random coil" value by similar electrostatic and hydrogen bonding interactions. However, unlike the capping His 18 in barnase, which lies over the end of an α-helix and therefore is aligned directly with its dipole moment, the side chain of His 156 lies well to the side of the α-helix in BCX. Also, the carbonyl of residue $i - 4$ (Ala 152) is hydrogen bonded to both the main-chain amide and imidazole ring of this histidine.

One unusual spectroscopic feature of His 156 is the absence of detectable ^{15}N resonances above pH ~ 6 (Fig. 2). This is likely due to interconversion between tautomeric forms on the timescale of intermediate exchange. Based on studies of model compounds, the $N^{\epsilon 2}H$ tautomer of a neutral histidine is preferred by ~5-fold over the $N^{\delta 1}H$ tautomer (Blomberg et al., 1977; Tanokura, 1983). However, hydrogen bonding to the carbonyl of Ala 152 requires protonation of $N^{\delta 1}$ (Campbell et al., 1993).[5] We speculate that, under basic conditions, such hydrogen bonding shifts the tautomeric equilibrium of His 156 closer to unity, and perhaps also perturbs the rate of proton transfer with the solvent. This extenuates the effect of intermediate exchange broadening as the populations of the two possible protonated forms of the imidazole become comparable (Cavanagh et al., 1996).

Solvent exchange of His 149

His 149 was identified initially in the NMR spectra of BCX due to the distinct resonance of its imidazole $^1H^{\epsilon 2}$ at 12.19 ppm. In general, this labile proton is not observable by ^{1}H-NMR methods due to rapid exchange with the solvent. However, many of the earliest NMR studies of proteins in H_2O solvents focused on "usually downfield shifted resonances" attributed to the nitrogen bonded protons of histidines (Markley, 1975). Examples include serine proteases (Robillard & Schulman, 1974; Markley, 1978) and heme proteins (Sheard et al., 1970; Redfield & Gupta, 1971), as well as ribonuclease A (Patel et al., 1972; Griffin et al., 1973), carbonic anhydrase (Gupta & Pesando, 1975), and superoxide dismutase (Stoesz et al., 1979). These histidines are often key active site residues or are involved in the ligation of metal ions (Feng et al., 1990).

At pH* 7.04 and 30 °C, the exchange rate of His 149 $^1H^{\epsilon 2}$ with bulk solvent is 4.0×10^{-5} s^{-1}, corresponding to a lifetime of ~ 7 h. This surprisingly slow exchange rate is comparable to those reported for the metal-ligated histidines in bovine superoxide dismutase (Stoesz et al., 1979). To the best of our knowledge, these are the only two proteins for which histidine exchange rates have been measured quantitatively. We estimate the exchange rate for the histidine imidazole protons in a random-coil polypeptide to be on the order of 10^2–10^3 s^{-1} at pH 7 (Englander & Kallenbach, 1984; Wüthrich, 1986; Creighton, 1993). Therefore, the $^1H^{\epsilon 2}$ of His 149 is protected from hydrogen exchange with the solvent by greater than 10^6-fold. This protection is attributed to the hydrogen bonding and solvent inaccessibility of the imidazole ring of the buried histidine (Fig. 7). It is intriguing that the $H^{\epsilon 2}$ of His 149 is hydrogen bonded to an internal water molecule in the X-ray structure of BCX, prompting the question as to the mechanism by which the hydrogen of this imidazole exchanges with bulk or possibly bound solvent. We are currently investigating this issue by characterizing in detail the kinetics of His 149 hydrogen exchange and the lifetime of the bound water molecule.

pK_a of His 149

His 149 exists in the neutral $N^{\epsilon 2}H$ tautomeric form between pH 9.3 and 2.3 at 30 °C (Fig. 2). Therefore, the pK_a of this histidine residue is <2.3. If we assume further that changes in chemical shift are detectable at pH values within ±0.5–1 units of the pK_a of an ionizable group, then the pK_a of His 149 is <1.8, as evident by the invariance of its ^{1}H- and ^{15}N-NMR spectra to changes in hydronium ion concentration. The abnormally low pK_a of His 149 undoubtedly reflects the buried hydrophobic environment of its imidazole ring in BCX. Although hydrogen bonded to a serine hydroxyl and a bound water, His 149 contacts several nonpolar residues, including Val 81, Val 98, Tyr 105, and Ile 144. The side-chain carboxyl of Asp 101 is also hydrogen bonded to the bound water, but is too far from His 149 to form a charge-stabilizing salt bridge ($d_{149N\epsilon 2\text{-}101O\delta 2}$ = 4.7 Å).

Abnormally low pK_a values (<2.8) have also been reported for histidine residues in cyclophilin and FK506 binding protein (Yu & Fesik, 1994). These imidazole side chains are, in effect, moderately strong acids, remaining deprotonated under all physiological conditions. In contrast, pK_a values of 9.1 and 10.4 have been measured for salt-bridged histidine side-chains in T4 lysozyme (Anderson et al., 1990) and superoxide dismutase (Stoesz et al., 1979), respectively (see also Liang & Abeles, 1987). These positively charged imidazolium side-chains are thus moderately strong bases. Remarkably, the acid dissociation constant of a histidine can vary by more than 10^8-fold depending on its structural and electrostatic environment within a protein!

BCX undergoes acid-induced denaturation in acidic solutions with pH values that are above the pK_a of His 149 (Fig. 2). This implies that His 149 is never protonated significantly when in the context of the folded xylanase. As discussed in detail by Anderson et al. (1993), the electrostatic contribution of an ionizable group toward the stability or instability of the native state of protein relative to the denatured state is reflected directly by the difference in the pK_a values of that group in these folded and unfolded states. Assuming a pK_a of 6.5 for a histidine in an unstructured polypeptide, the presence of neutral His 149 destabilizes folded BCX by ~5.5 kcal/mol at pH 2.5 and 30 °C. However, under biologically relevant conditions near neutral pH, His 149 is deprotonated in both native and denatured BCX. Thus, no significant energetic penalty results from the burial of its side chain and, under these conditions, His 149 can contribute favorably to the stability of the folded protein through hydrogen bonding, van der Waals, and possibly aromatic–aromatic interactions. Consistent with this argument, calorimetric studies have shown that the midpoint temperature for the thermal denaturation of BCX is maximal near pH 5 and drops sharply with increased solution acidity (Davoodi et al., 1995). We are currently measuring the pK_a values of all the glutamic and aspartic acid groups in BCX in order to understand in detail the pH-dependence of the stability of this enzyme (McIntosh et al., 1996).

[5] The crystal structure of BCX was solved at pH 7.3.

Structural conservation and site-directed mutagenesis

His 149, Tyr 105, and Ser 130 are conserved completely in all family G xylanases. Furthermore, the hydrogen bonding interactions between these residues and a buried water are also found in the reported crystal structures of the homologous *T. harzianum* and *T. reesei* I and II xylanases (Campbell et al., 1993; Törrönen et al., 1994; Törrönen & Rouvinen, 1995). These side chains are located on the "backside" of the enzyme, relative to the active site cleft, and thus are likely to fulfill important roles in establishing the structural stability of these xylanases, as opposed to having a direct catalytic function.

To probe the role played by His 149, site-directed mutagenesis was used to substitute phenylalanine (H149F) and glutamine (H149Q) at this position. Preliminary measurements demonstrated that, at 40 °C, the two mutant proteins have the same specific activity as the wild-type BCX (data not shown). As expected, the amino acid replacements do not alter significantly the active site of the enzyme. However, after a 10-min incubation period at 55 °C, both mutant xylanases retained only 10% of their catalytic activity. In constrast, the wild-type protein showed no decrease in activity even after 1 h under these conditions (50 mM NaCl, 50 mM MES, pH 6.0) (Wakarchuk et al., 1994b). Therefore, the substitutions H149F and H149Q lead to a reduction in the stability of folded BCX as is evident by these measurements of its irreversible thermal denaturation. Based on the crystal structure of the wild-type xylanase, we postulate that this reduction in stability results from unsatisfied hydrogen bonds to the buried polar groups of Ser 130 and, if still present, the internal water molecule, combined with altered van der Waals contacts of the phenylalanine and glutamine side chains to the residues surrounding position 149. The importance of these interactions toward stabilizing the folded structure of BCX are reflected by the slow hydrogen exchange rate and exceptionally low pK_a value observed for the imidazole side chain of His 149 in the wild-type enzyme.

Materials and methods

Protein preparation

The gene encoding BCX was cloned into the pCW plasmid system under control of an inducible tac promoter (Sung et al., 1993; Wakarchuk et al., 1994a). Unlabeled and biosynthetically ^{15}N- and $^{13}C/^{15}N$-labeled BCX were produced in the prototrophic *Escherichia coli* strain 594, and purified by ion-exchange chromatography, as described previously (Sung et al., 1993; Plesniak et al., 1996). Unless stated otherwise, samples used for NMR analyses were 0.8–1.0 mM BCX in 25 mM sodium d_3-acetate, 0.02% sodium azide, 90% H_2O/10% D_2O at pH* 5.8. The pH of the protein was lowered during the titration experiments by the addition of microliter aliquots of 0.1 M HCl and, when necessary, raised by dialysis against alkaline sample buffer to avoid possible aggregation resulting from the direct addition of base. The sample pH* was measured at room temperature using an Ingold microelectrode.

NMR spectroscopy

NMR spectra were recorded at 30 °C using a Varian Unity Spectrometer operating at 500 MHz for protons, and processed off-line using FELIX v2.30 software (Biosym Inc., San Diego, CA). ^{15}N-NMR spectra were acquired with a 10-mm broadband probe and all other data collected with a 5-mm triple resonance $^{15}N/^{13}C/^{1}H$ probe containing a single shielded gradient coil. ^{1}H and ^{13}C were referenced to an external sample of DSS at 0.00 ppm for both nuclei, and ^{15}N to an external sample of 2.9 M $^{15}NH_4Cl$ in 1 M HCl at 29.43 ppm (Levy & Lichter, 1979). This latter reference yields ^{15}N chemical shifts 1.6 ppm greater than those obtained using liquid NH_3 (Wishart et al., 1995).

Directly observed one-dimensional ^{15}N-NMR spectra of ^{15}N-enriched BCX were recorded using a ~50 degree ^{15}N pulse, a spectral width of 282 ppm, an acquisition period of 287 ms, and a total recycle delay of ~1.8 s. Broadband proton decoupling during acquisition was achieved using a GARP sequence, applied at 9.1 ppm with a field strength of 900 Hz. Approximately 5,000 transients were accumulated in 2–3 h to yield sufficient signal-to-noise in the final spectra.

The ^{1}H-^{15}N HSQC spectrum of ^{15}N-enriched BCX was recorded using spectral widths of 8,064 Hz (16.1 ppm) and 6,944 Hz (137 ppm), and acquisition times of 127 ms and 37 ms in ^{1}H and ^{15}N, respectively, to encompass the entire chemical shift range of each nuclei. The signal from water was reduced by selective saturation, and broadband GARP decoupling at a field strength of 1,800 Hz was applied to ^{15}N during acquisition.

The ^{1}H-^{15}N HMBC spectrum of uniformly $^{13}C/^{15}N$-labeled BCX was collected in a mixed-mode using spectral widths of 12,500 Hz (25 ppm) and 4,560 Hz (90 ppm), and acquisition times of 82 ms and 56.1 ms in ^{1}H and ^{15}N, respectively (Bax & Marion, 1988). The ^{15}N transmitter was set at 210 ppm, and signals from the amide and guanido groups were aliased to the middle and edge of the spectrum, respectively. A delay of 22 ms was used to detect the weak two- and three-bond ^{1}H-^{15}N correlations while minimizing the signal due to directly bonded ^{1}H-^{15}N pairs (Pelton et al., 1993). The signal from water was reduced by selective saturation, and broadband GARP decoupling at a field strength of 1,850 Hz was applied to the ^{13}C nuclei in aromatic region (124.5 ppm) during both t_1 and t_2 periods. The spectrum was processed using skewed shifted sinebell apodization in both dimensions. The ^{1}H-^{15}N HMBC spectrum was recorded on a ^{13}C- and ^{15}N-enriched sample to allow a precise alignment with the ^{1}H-^{13}C HSQC spectrum of BCX.

The constant-time ^{1}H-^{13}C HSQC spectrum of the aromatic region of uniformly $^{13}C/^{15}N$-enriched BCX was recorded using spectral widths of 6,250 Hz (12.5 ppm) and 6,200 Hz (49 ppm), and acquisition times of 164 ms and 16.3 ms in ^{1}H and ^{13}C, respectively (Santoro & King, 1992; Vuister & Bax, 1992). The ^{13}C transmitter was set at 124.5 ppm. A total constant-time delay of 16.7 ms was chosen assuming a $^{1}J_{CC} \sim 60$ Hz for the aromatic ring carbons. Decoupling of the aromatic ^{15}N during t_1 was accomplished by GARP decoupling centered at 151 ppm and with a field strength of 790 Hz. The signal from water was eliminated using the gradient accessory as a homospoil (Wider & Wüthrich, 1993). The spectra were processed using mirror image linear prediction in the ^{13}C dimension (Zhu & Bax, 1992).

The ^{1}H-^{13}C (Hβ)Cβ(CγCδ)Hδ spectrum of uniformly ^{13}C- and ^{15}N-enriched BCX was recorded using spectral widths of 6,250 Hz (12.5 ppm) and 4,000 Hz (32 ppm), and acquisition times of 82 ms and 8 ms in ^{1}H and ^{13}C, respectively (Yamazaki et al., 1993). The ^{13}C transmitter was set at 37 ppm. Mirror image linear prediction was used during processing of the data for the constant-time ^{13}C dimension.

Hydrogen-deuterium exchange

The kinetics of hydrogen-deuterium exchange of His 149 were measured by transferring BCX into 99% D_2O buffer, containing

15 mM sodium d_3-acetate, 15 mM sodium phosphate, and 0.01% sodium azide, using a Sephadex G25 medium spin column. The Sephadex was swollen in the D_2O buffer overnight and packed in a 3 mL Quik-Sep (Isolab, Inc., Akron, OH) column using a swinging-bucket centrifuge spun at 6,000 rpm for 2 min. BCX in 600 μL of H_2O buffer was loaded on the top of the column, followed immediately by centrifugation at the same speed for 2 min. The protein in D_2O buffer was placed in a dry NMR tube and, after ~5 min to equilibrate at 30 °C in the magnet, a series of one-dimensional ^{1}H-NMR spectra, each signal averaged over 10 min, were collected. The sample pH was measured at room temperature after completion of the experiment. The exchange rate (k_{ex}) was determined using the program Kaleidagraph (Synergy Software) by fitting the height (I_t) of the $^1H^{\epsilon 2}$ peak versus time to the expression $I_t = I_o e^{-(kex)t} + I_\infty$, where I_∞ accounts for the effect of residual HDO.

Note added in proof

J.L. Markley and W.M. Westler (*Biochemistry 35*:11092–11097, 1996) reported recently exchange rates for the catalytic triad histidine of bovine chymotrypsin A.

Acknowledgments

We thank Toshio Yamazaki and Lewis Kay for invaluable discussions and for providing NMR pulse sequences.

References

Anderson DE, Becktel WJ, Dahlquist FW. 1990. pH-induced denaturation of proteins: A single salt bridge contributes 3–5 kcal/mol to the free energy of folding of T4 lysozyme. *Biochemistry 29*:2403–2408.

Anderson DE, Lu J, McIntosh LP, Dahlquist FW. 1993. The folding, stability and dynamics of T4 lysozyme: A perspective using nuclear magnetic resonance. In: Clore GM, Gronenborn AM, eds. *NMR of proteins*. London: MacMillan Press. pp 258–304.

Armstrong KM, Fairman R, Baldwin RL. 1993. The (*i*, *i* + 4) Phe-His interaction studied in an alanine-based α-helix. *J Mol Biol 230*:284–291.

Bachovchin WW. 1986. ^{15}N NMR spectroscopy of hydrogen-bonding interactions in the active site of serine proteases: Evidence for a moving histidine mechanism. *Biochemistry 25*:7751–7759.

Bax A, Marion D. 1988. Improved resolution and sensitivity in ^{1}H-detected multiple-bond correlation spectroscopy. *J Magn Res 78*:186–191.

Blomberg F, Maurer W, Rüterjans H. 1977. Nuclear magnetic resonance investigation of ^{15}N-labeled histidine in aqueous solution. *J Am Chem Soc 99*:8149–8159.

Blomberg F, Rüterjans H. 1983. Nitrogen-15 NMR in biological systems. *Biological Magnetic Resonance 5*:21–73.

Bundi A, Wüthrich K. 1979. ^{1}H-NMR parameters of the common amino acid residues measured in aqueous solutions of the linear tetrapeptides H-Gly-Gly-X-L-Ala-OH. *Biopolymers 18*:285–297.

Burley SK, Petsko GA. 1988. Weakly polar interactions in proteins. *Adv Protein Chem 39*:125–189.

Campbell R, Rose D, Wakarchuk W, To R, Sung W, Yaguchi M. 1993. A comparison of the structures of the 20 kD xylanases from *Trichoderma harzianum* and *Bacillus circulans*. In: Suominen P, Reinikainen T, eds. *Proceedings of the second TRICEL symposium on Trichoderma reesei cellulases and other hydrolyases. Espoo, Finland*. Helsinki: Foundation for Biotechnological and Industrial Fermentation Research. pp 63–77.

Cavanagh J, Fairbrother WJ, Palmer AG, Skelton NJ. 1996. *Protein NMR spectroscopy: Principles and practice*. Toronto: Academic Press.

Coughlan MP, Hazlewood GP. 1993. β-1,4-D-Xylan-degrading enzyme systems: Biochemistry, molecular biology and applications. *Biotechnol Appl Biochem 17*:259–289.

Creighton TE. 1993. *Proteins: Structures and molecular properties, 2nd ed.* New York: W.H. Freeman & Co.

Davies G, Henrissat B. 1995. Structures and mechanisms of glycosyl hydrolases. *Structure 3*:853–859.

Davoodi J, Wakarchuk WW, Campbell RL, Carey PR, Surewicz WK. 1995. Abnormally high pK_a of an active-site glutamic acid residue in *Bacillus circulans* xylanase—The role of electrostatic interactions. *Eur J Biochem 232*:839–843.

Englander SW, Kallenbach NR. 1984. Hydrogen exchange and structural dynamics of proteins and nucleic acids. *Quart Rev Biophys 16*:521–655.

Evans S. 1993. SETOR: Hardware lighted three-dimensional solid model representations of macromolecules. *J Mol Graphics 11*:134–138.

Feng Y, Röder H, Englander SW. 1990. Assignment of paramagnetically shifted resonances in the ^{1}H NMR spectrum of horse ferricytochrome *c*. *Biophys J 57*:15–22.

Gebler J, Gilkes NR, Claeyssens M, Wilson DB, Beguin P, Wakarchuk W, Kilburn DG, Miller RCJ, Warren RAJ, Withers SG. 1992. Stereoselective hydrolysis catalysed by related β-1,4-glucanases and β-1,4-xylanases. *J Biol Chem 267*:12259–12262.

Gilkes NR, Henrissat B, Kilburn DG, Miller RC Jr, Warren RAJ. 1991. Domains in microbial beta-1,4-glycanases: Sequence conservation, function, and enzyme families. *Microbiol Rev 55*:303–315.

Griffin JH, Cohen JS, Schechter AN. 1973. The assignment of an exchangeable low-field NH proton resonance of ribonuclease A to the active-site histidine-119. *Biochemistry 12*:2096–2099.

Gupta RK, Pesando JM. 1975. Magnetic resonance study of exchangeable protons in human carbonic anhydrase. *J Biol Chem 250*:2630–2634.

Henrissat B, Bairoch A. 1993. New families in the classification of glycosyl hydrolases based on amino acid sequence similarities. *Biochem J 293*:781–788.

Lawson SL, Wakarchuk WW, Withers SG. 1996. Effects of both shortening and lengthening the active site nucleophile in *Bacillus circulans* xylanase on catalytic activity. *Biochemistry 35*:10110–10118.

Levy GC, Lichter RL. 1979. *Nitrogen-15 nuclear magnetic resonance spectroscopy*. New York: Wiley & Sons.

Liang TC, Abeles RH. 1987. Complex of α-chymotrypsin and N-acetyl-L-leucyl-L-phenyalanyl trifluoromethyl ketone: Structural studies with NMR spectroscopy. *Biochemistry 2b*:7603–7608.

Markley JL. 1975. Observation of histidine residues in proteins by means of NMR spectroscopy. *Acc Chem Res 8*:70–80.

Markley JL. 1978. Hydrogen bonds in serine proteinases and their complexes with protein proteinase inhibitors. Protein nuclear magnetic resonance studies. *Biochemistry 22*:4648–4656.

McIntosh LP, Hand G, Johnson PE, Joshi MD, Körner M, Plesniak LA, Ziser L, Wakarchuk WW, Withers SG. 1996. The pK_a of the general acid/base carboxyl group of a glycosidase cycles during catalysis: A ^{13}C-NMR study of *Bacillus circulans* xylanase. *Biochemistry 35*:9958–9966.

Miao S, Ziser L, Aebersold R, Withers SG. 1994. Identification of glutamic acid 78 as the active site nucleophile in *Bacillus subtilis* xylanase using electrospray tandem mass spectroscopy. *Biochemistry 33*:7027–7032.

Otting G, Liepinsh E, Wüthrich K. 1991. Protein hydration in aqueous solution. *Science 254*:974–980.

Otting G, Wüthrich K. 1989. Studies of protein hydration in aqueous solution by direct NMR observation of individual protein-bound water molecules. *J Am Chem Soc 111*:1871–1875.

Paice MG, Bourbonnais R, Desrochers M, Jurasek L, Yaguchi M. 1986. A xylanase from *Bacillus subtilis*: Nucleotide sequence and comparison with *B. pumilus* gene. *Arch Microbiol 144*:201–206.

Patel DJ, Woodward CK, Bovey FA. 1972. Proton nuclear magnetic resonance studies of ribonuclease A in H_2O. *Proc Natl Acad Sci USA 69*:599–602.

Pelton JG, Torchia DA, Meadow ND, Roseman S. 1993. Tautomeric states of the active-site histidines of phosphorylated and unphosphorylated III^{Glc}, a signal-transducing protein from *Escherichia coli*, using two-dimensional heteronuclear NMR techniques. *Protein Sci 2*:543–558.

Plesniak LA, Wakarchuk WW, McIntosh LP. 1996. Secondary structure and NMR assignments of *Bacillus circulans* xylanase. *Protein Sci 5*:1118–1135.

Redfield AG, Gupta RK. 1971. Pulsed Fourier-transform NMR spectrometer for use with H_2O solutions. *J Chem Phys 54*:1418–1419.

Richardson JS, Richardson DC. 1988. Amino acid preferences for specific locations at the ends of α-helices. *Science 240*:1648–1652.

Richarz R, Wüthrich K. 1978. Carbon-13 NMR chemical shifts of the common amino acid residues measured in aqueous solutions of the linear tetrapeptides H-Gly-Gly-X-L-Ala-OH. *Biopolymers 17*:2133–2141.

Robillard G, Schulman RG. 1974. High resolution nuclear magnetic resonance studies of the active site of chymotrypsin. *J Mol Biol 86*:519–540.

Sancho J, Serrano L, Fersht AR. 1992. Histidine residues at the N- and C-termini of α-helices: Perturbed pK_as and protein stability. *Biochemistry 31*:2253–2258.

Santoro J, King GC. 1992. A constant-time 2D Overbodenhausen experiment for inverse correlation of isotopically enriched species. *J Magn Reson 97*: 202–207.

Sheard B, Yamane T, Shulman RG. 1970. Nuclear magnetic resonance study of

cyanoferrimyoglobin; identification of pseudocontact shifts. *J Mol Biol 53*: 35–48.

Sklenár V, Bax A. 1987. Spin-echo water suppression for the generation of pure-phase two-dimensional NMR spectra. *J Magn Reson 74*:469–479.

Stoesz JD, Malinowski DP, Redfield AG. 1979. Nuclear magnetic resonance study of solvent exchange and nuclear Overhauser effect of the histidine protons of bovine superoxide dismutase. *Biochemistry 18*:4669–4675.

Sung WL, Luk CK, Zahab DM, Wakarchuk W. 1993. Overexpression and purification of the *Bacillus subtilis* and *Bacillus circulans* xylanases in *Escherichia coli*. *Prot Express Purif 4*:200–216.

Tanokura M. 1983. Microscopic pK values and molar ratios of tautomers in histidine-containing peptides. *Biochem Biophys Acta 742*:576–585.

Törrönen A, Harkki A, Rouvinen J. 1994. Three-dimensional structure of endo-1,4-β-xyanase II from *Trichoderma reesei*: Two conformational states in the active site. *EMBO J 13*:2943–2501.

Törrönen A, Rouvinen J. 1995. Structural comparison of two major endo-1,4-xylanases from *Trichoderma reesei*. *Biochemistry 34*:847–856.

van Dijk AA, Scheek RM, Dijkstra K, Wolters GK, Robillard GT. 1992. Characterization of the protonation and hydrogen bonding state of the histidine residues in IIA^{mtl}, a domain of the phosphoenolpyruvate-dependent mannitol-specific transport protein. *Biochemistry 31*:9063–9072.

Vuister GW, Bax A. 1992. Resolution enhancement and spectral editing of uniformly ^{13}C-enriched proteins by homonuclear broadband ^{13}C decoupling. *J Magn Reson 98*:428–435.

Wakarchuk WW, Campbell RL, Sung WL, Davoodi J, Yaguchi M. 1994a. Mutational and crystallographic analyses of the active site residues of the *Bacillus circulans* xylanase. *Protein Sci 3*:467–475.

Wakarchuk WW, Methot N, Lanthier P, Sung W, Seligy V, Yaguchi M, To R, Campbell R, Rose D. 1992. The 20 kD xylanase of *Bacillus subtilis*: A structure/function analysis. In: Visser J et al., eds. *Xylan and xylanases*. Amsterdam: Elsevier Science B.V. pp 439–442.

Wakarchuk WW, Sung WL, Campbell RL, Cunnigham A, Watson DC, Yaguchi M. 1994b. Thermostabilization of the *Bacillus subtilis* xylanase by the introduction of disulfide bonds. *Protein Eng 7*:1379–1386.

Wider G, Wüthrich K. 1993. A simple experimental scheme using pulsed field gradients for coherence-pathway rejection and solvent suppression in phase-sensitive heteronuclear correlation spectra. *J Magn Reson 102*:239–241.

Wishart DS, Bigam CG, Yao J, Abildgaard F, Dyson HJ, Oldfield E, Markley JL, Sykes BD. 1995. ^{1}H, ^{13}C and ^{15}N chemical shift referencing in biomolecular NMR. *J Biol NMR 6*:135–140.

Witanowski M, Stefaniak L, Webb GA. 1986. Nitrogen NMR spectroscopy. *Annu Rep NMR Spectroscopy 18*:1–763.

Wu X, Westler WM, Markley JL. 1984. The assignment of imidazolium N-^{1}H peaks in the ^{1}H-NMR spectum of a protein by one- and two-dimensional NOE experiments. *J Magn Reson 59*:524–529.

Wüthrich K. 1986. *NMR of proteins and nucleic acids*. New York: Wiley & Sons.

Yamazaki T, Foreman-Kay JD, Kay L. 1993. Two-dimensional NMR experiments for correlating $^{13}C^{\beta}$ and $^{1}H^{\delta/\epsilon}$ chemical shifts of aromatic residues in ^{13}C-labelled proteins via scalar couplings. *J Am Chem Soc 115*:11054–11055.

Yu L, Fesik SW. 1994. pH titration of the histidine residues of cyclophilin and FK506 binding protein in the absence and presence of immunosuppressant ligands. *Biochem Biophys Acta 1209*:24–32.

Zhong S, Haghjoo K, Kettner C, Jordan F. 1995. Proton magnetic resonance studies of the active center histidine of chymotrypsin complexed to peptideboronic acids: Solvent accessibility to the N^{δ} and N^{ϵ} sites can differentiate slow-binding and rapidly reversible inhibitors. *J Am Chem Soc 117*:7048–7055.

Zhu G, Bax A. 1992. Improved linear prediction of damped NMR signals using modified "forward-backward" linear prediction. *J Magn Reson 100*: 202–207.